COMITATO NAZIONALE PER L'ENERGIA NUCLEARE
Laboratori Nazionali di Frascati

LNF-67/32
10 Maggio 1967

G. Bologna: ON THE EXTENT TO WHICH COHERENT BREMSSTRAHLUNG FROM CRYSTALS CAN BE MONOCHROMATIZED. -

(Nota interna: n. 363)

Servizio Documentazione
dei Laboratori Nazionali di Frascati del CNEN
Casella Postale 70 - Frascati (Roma)

Laboratori Nazionali di Frascati del CNEN
Servizio Documentazione

LNF - 67/32

Nota interna : n. 363
10 Maggio 1967

G. Bologna: ON THE EXTENT TO WHICH COHERENT BREMSSTRAHLUNG FROM CRYSTALS CAN BE MONOCHROMATIZED.

High energy bremsstrahlung spectra showing several linearly polarized spikes, like those of fig. 1 (dot-dash curves), were first obtained at the Frascati 1-GeV electronsynchrotron by using a single crystal as a radiator(1).

The reason of such non-Bethe-Heitler behaviour of bremsstrahlung process is seen to be due to the restricted range of crystal recoils. As far as Laue law is obeyed, only those recoils are permitted which are normal to a set of crystal lattice planes.

Now a further restriction of the allowed recoils can be kinematically obtained, as proposed by Mozley and De Wire(2), by a strong collimation of the photon beam. As a result, the spikes are sharpened as shown for instance by the dashed curves of fig. 1. Essentially monoenergetic γ-ray beams with a linear polarization close to 100% can in principles be obtained in this way.

Unfortunately both the divergence and the multiple scattering of primary electrons play a major role in masking the effect of collimation, so that monoenergetic bremsstrahlung was not observed till now.

As such beams can be of importance for high energy particle physics, a work was undertaken by the author in order to investigate what degree of monochromaticity can be preserved by considering the actual experimental conditions.

Typical results, to be explained in what follows, are shown by the continuous curves of figs. 1 and 2, as well as by the dashed curve of fig. 2.

The following steps were accomplished:

1) Evaluation of the coherent and polarized bremsstrahlung cross section, differential both in angles and energy. In previous works[1, 3, 4] cross sections differential in energy only were given.

2) Folding of the differential cross section with the electron distribution for multiple scattering and beam divergence.

3) Integration, extended to the angular region accepted by the collimator, of the expressions thus obtained.

4) Best choice of the crystal.

Several points are not considered. For instance, the influence of the source extension is not examined yet, because that makes the problem much more involved; on the other hand this effect can in a sense be simulated by suitably enlarging the collimator. Other points not considered are the technical difficulties in obtaining thin single crystals, like those needed here, and the related problem of crystal defects.

The results we present here were obtained by using Born approximation, as well as high energy and small angle approximation. The following units are used: mc^2, the rest energy of the electron, for energies; mc for linear momenta; $\lambda_c = h/mc$, the electron Compton wave length, for lengths.

Let $\vec{p}_1$ be the momentum of the incoming electron; $E_1 \simeq p_1 \gg 1$ be its energy; $E_2 \gg 1$ be the energy of the outgoing electron; $\vec{k}$ be the momentum of the emitted photon, $x = k/E_1$ its fractional energy; $\vec{q}$ be the momentum transferred to the atom, q_z and $q_\perp$ the components of $\vec{q}$ along and transverse to $\vec{p}_1$, δ the minimum momentum transfer; U be the emission angle of the photon (angle between $\vec{k}$ and $\vec{p}_1$) in $1/E_1$ units ($U/E_1 \ll \ll 1$ radian), γ the angle of the planes $(\vec{p}_1, \vec{q})$ and $(\vec{p}_1, \vec{k})$. We have

$$\delta = \frac{k}{2E_1E_2} = \frac{x}{2E_1(1-x)}$$

$$q_z = \delta(1+U^2) - 2\delta U q_\perp \cos\gamma + \frac{q_\perp^2}{2E_2} . \tag{1}$$

The last equation represents a parabolic surface in $\vec{q}$ space. The relevant term on the right side of eq. (1) is the first one (the maximally contributing values of q and U for bremsstrahlung are of the order of 10^{-2} and 1, respectively; furthermore we assumed $E_2 \gg 1$). We have thus

$$q_z \simeq \delta(1+U^2); \tag{2}$$

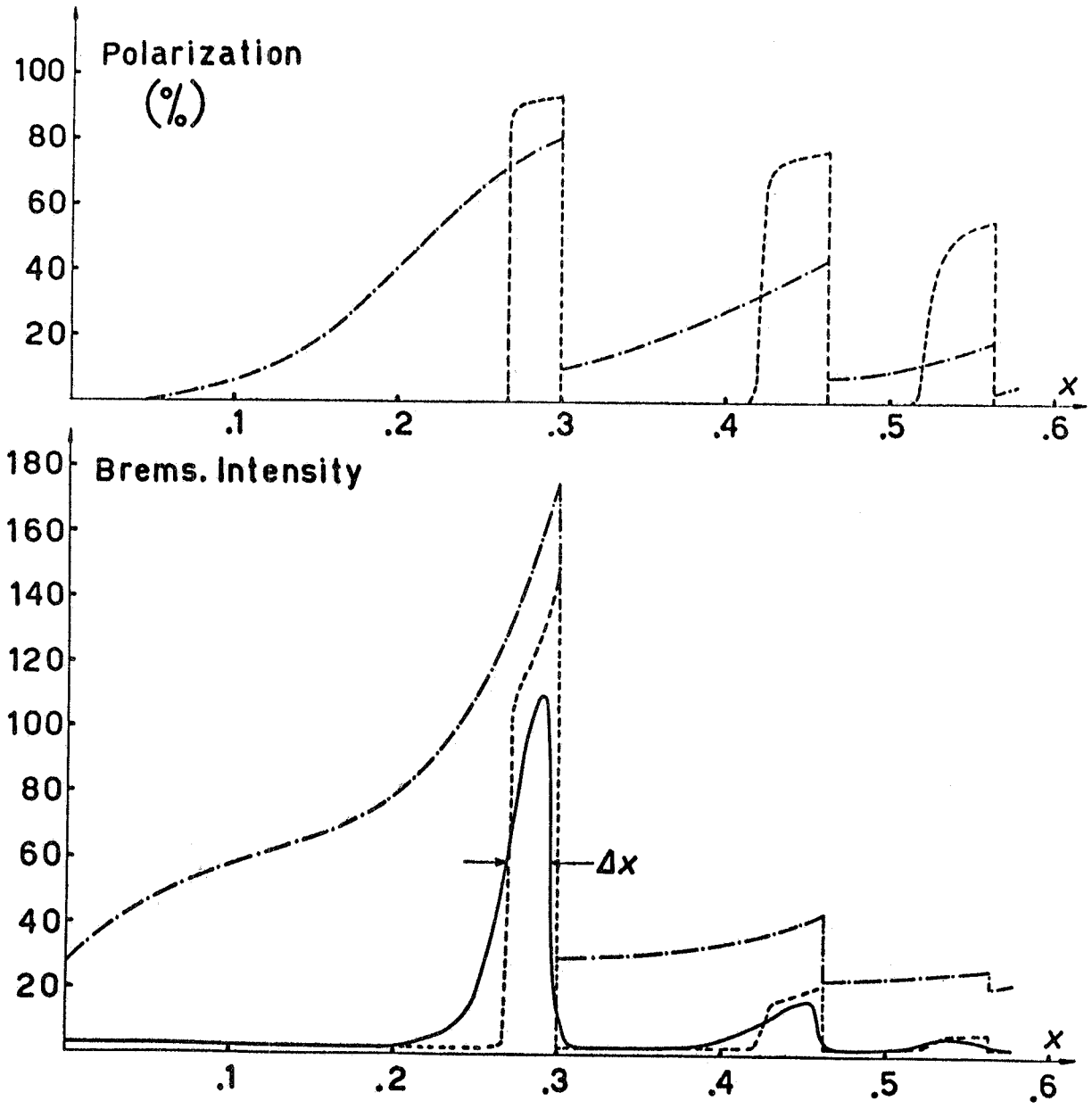

FIG. 1 - Bremsstrahlung intensity $x(d\sigma/dx)/(Z^2\sigma_0 N)$ and polarization $[d\sigma_\perp^{(i)} - d\sigma_\parallel^{(i)}]/d\sigma$ from a single crystal of beryllium, versus photon fractional energy $x = k/E_1$. $mc^2E_1 = 6\,GeV$; $\vec{b}_1 \equiv [1\bar{2}10]$; $\vec{b}_2 \equiv [10\bar{1}0]$; $b_3 \equiv [0001]$; $\alpha = \beta = 1.5^o$; $\theta/E_1 = 51.3$ mrad. Dot-dash curves: no collimation, no scattering, no beam divergence. Dashed curves: $U_o/E_1 = 3.4 \times 10^{-5}$ rad; no scattering; no beam divergence; $\Delta x/x = 11\%$. Continuous curve: same U_o; $T = 9.25 \times 10^{-3}$ gr/cm^2; no beam divergence; same $\Delta x/x$.

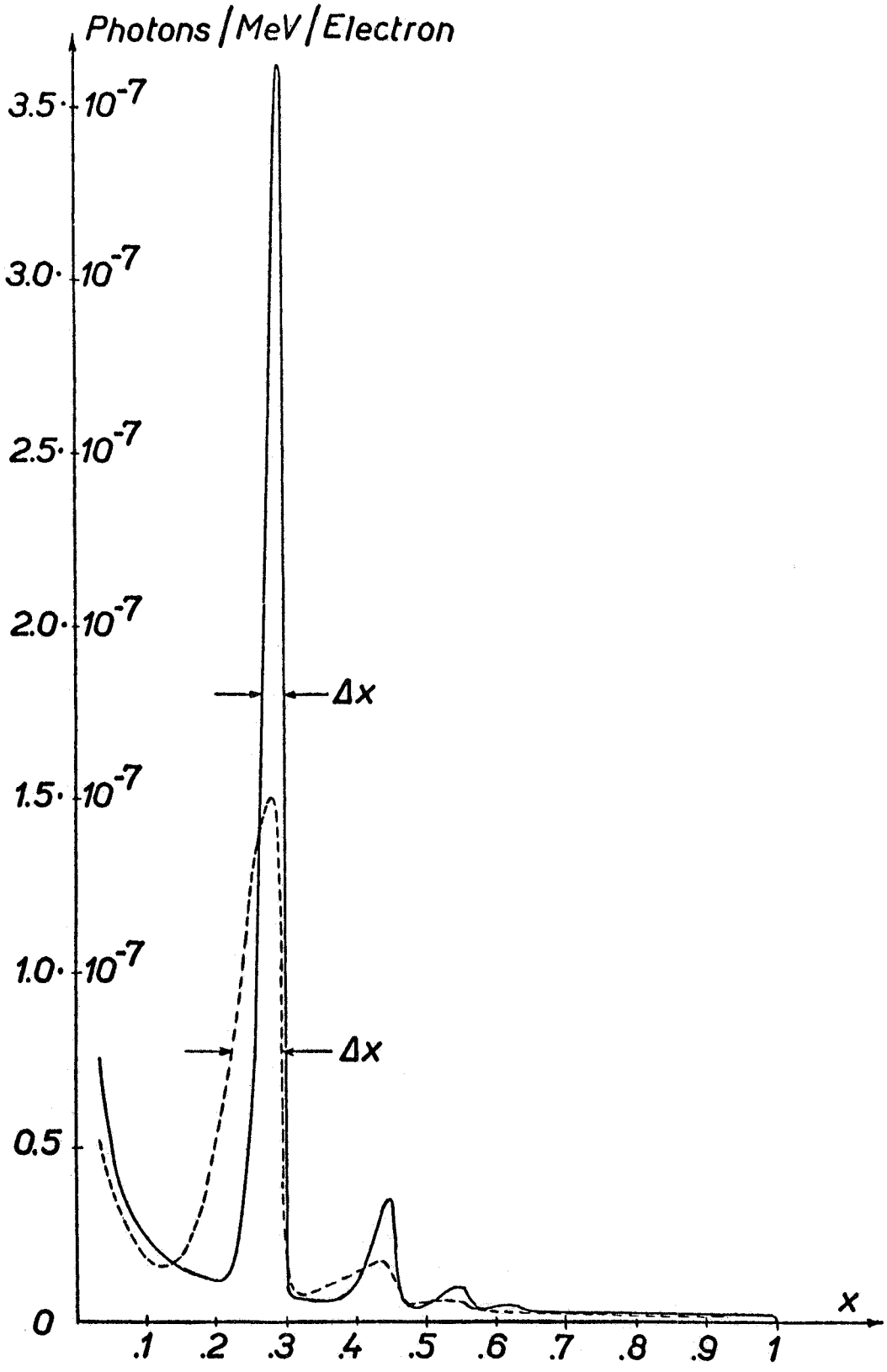

FIG. 2 - Number of photons per MeV emitted by an electron, versus x. Conditions for the continuous curve are the same as for continuous curve of fig. 1 are. Dashed curve: beam divergence $\omega_o/E_1 = 4.3 \times 10^{-5}$ rad. Other conditions are unchanged ($\omega_M(T)/E_1 = 2.1 \times 10^{-5}$ rad); $\Delta x/x = 25\%$.

the paraboloid approximately degenerates in a plane perpendicular to $\vec{p}_1$, having a distance $\delta(1+U^2)$ from the origin.

If a round collimator is placed at the center of the bremsstrahlung beam, U assumes all the values between zero and a maximum value U_o; thus the allowed kinematical region assumes the well known shape of Überall's "pancake"(5); this pancake, which is perpendicular to $\vec{p}_1$, has a distance δ from the origin and a thickness δU_o^2.

Let now $\vec{b}_1$, $\vec{b}_2$, $\vec{b}_3$ be three orthogonal reference axes (in general not coincident with the basis axes of the crystal), chosen in such a way that the angle between $\vec{p}_1$ and $\vec{b}_1$ is $\theta/E_o \ll 1$ radian. This angle plays a fundamental role in what follows; with this choice many equations simplify.

If we take the origin of $\vec{q}$ space coincident with that of $\vec{b}_1$, $\vec{b}_2$, $\vec{b}_3$ and consider the surface of eq. (1), we have a situation which is the exact analogous of that for coherent scattering of X-rays. If $\vec{g}$ is a vector of the reciprocal lattice space, the coherent emission of a photon only takes place when $\vec{q}=\vec{g}$(5), which is the same as the Laue law. With a geometrical picture we can say the photon is emitted at the angle U when the paraboloid (1) passes through a reciprocal lattice point. This "coherence"paraboloid thus plays the same role as the Ewald sphere plays for X-ray scattering.

By calling g_i the components of $\vec{g}$ along $\vec{b}_i$, α the angle of the planes $(\vec{b}_1, \vec{b}_2)$ and $(\vec{b}_1, \vec{p}_1)$, β the angle of $(\vec{b}_1, \vec{b}_2)$ and $(\vec{b}_1, \vec{\varepsilon})$, where $\vec{\varepsilon}$ is the direction of the photon polarization, ψ the angle of $(\vec{p}_1, \vec{k})$ and $(\vec{p}_1, \vec{\varepsilon})$ (all oriented from the former to the latter plane), the condition $\vec{q}=\vec{g}$ becomes

$$(3)\quad \begin{cases} q_z = g_1 + \dfrac{\theta}{E_1}(g_2\cos\alpha + g_3\sin\alpha); \qquad q_\perp^2 = g_2^2 + g_3^2 \\ q_\perp \cos\gamma = -\, g_2\cos(\psi-\beta) + g_3\sin(\psi-\beta). \end{cases}$$

These are to be inserted in eq. (1) in order to obtain the emission angles U, ψ of the photon, when existing. These angles are completely determined by each reciprocal lattice point (viz., by each direct lattice set of parallel planes) and by the electron and photon energies. The situation is thus completely different with respect to incoherent bremsstrahlung.

Going back to the collimated bremsstrahlung beam, we can qualitatively reproduce the behaviour of the dashed spectrum of fig. 1, for which $U_o = 0.4$, by giving the pancake a translation along $\vec{p}_1$ and looking at the points of the reciprocal lattice which escape or enter the pancake. The points which give the relevant contribution are those of the plane $(\vec{b}_2, \vec{b}_3)$ through the origin(5), for which $g_1 = 0$. From eq. (2) the range Δx for which a lattice point is contained within the pancake is easily evaluated. The "line width" at $x = 0.3$ in fig. 1 is thus approximately

$$\frac{\Delta x}{x} = (1 - x)\, U_o^2 = 11\%. \tag{4}$$

Let us call now $d\sigma_{\parallel}^{(i)}$ and $d\sigma_{\perp}^{(i)}$ the interference part of the differential cross section for bremsstrahlung with polarization $\vec{\varepsilon}$ parallel and perpendicular to a fixed reference plane (this can be either $(\vec{p}_1, \vec{\varepsilon})$ or $(\vec{b}_1, \vec{\varepsilon})$, as $\vec{p}_1$ and $\vec{b}_1$ are nearly parallel). The position of the reference plane with respect to the crystal is conveniently determined by the angle β already defined.

In terms of β and $\vec{g}$ the angle φ between the planes $(\vec{p}_1, \vec{q})$ and $(\vec{p}_1, \vec{\varepsilon})$ or the planes $(\vec{b}_1, \vec{q})$ and $(\vec{b}_1, \vec{\varepsilon})$ is given by

$$\cos 2\varphi = \frac{(g_2^2 - g_3^2)\cos 2\beta + 2\, g_2\, g_3 \sin 2\beta}{g_2^2 + g_3^2} \,. \tag{5}$$

By considering May's differential cross section for polarized bremsstrahlung[6] and by introducing the crystal interference factor[5], we have found for the cross sections relative to the plane through the origin ($g_1 = 0$)

$$\begin{cases} d\sigma_{\perp}^{(i)} + d\sigma_{\parallel}^{(i)} = d\sigma^{(i)} = \dfrac{\sigma_o N}{x}\, I(U, \psi, x, E_1)\, \delta(U^2 - W^2)\, dU^2\, d\psi\, dx \\ d\sigma_{\perp}^{(i)} - d\sigma_{\parallel}^{(i)} = \dfrac{\sigma_o N}{x}\, I_-(U, \psi, x, E_1)\, \delta(U^2 - W^2)\, dU^2\, d\psi\, dx \,, \end{cases} \tag{6}$$

where $\sigma_o = (e^2/\hbar c)(e^2/mc^2)^2 = 5.78 \times 10^{-28}\ \mathrm{cm}^2$; N is the total number of atoms of the crystal; $\delta(U^2 - W^2)$ is the Dirac δ-function of the argument $U^2 - W^2$, and W^2 is the value of U^2 obtained from eq. (1) for $\vec{q} = \vec{g}$, viz. by using eqs. (3). After substitution we obtain

$$\begin{cases} J(U, \psi, x) = \dfrac{I(U, \psi, x, E_1)}{E_1} = \\ = \left[1 + (1-x)^2\right] D\, \phi_1(U, \psi, x) - \dfrac{2}{3}(1-x)\, D^2\, \phi_2(U, \psi, x) \\ J_-(U, \psi, x) = \dfrac{I_-(U, \psi, x, E_1)}{E_1} = 2(1-x)\, D\, \phi_3(U, \psi, x) \,, \end{cases} \tag{7}$$

where

$$D = \delta E_1 = \frac{x}{2(1-x)} \,;$$

J, J_-, ϕ_1, ϕ_2, ϕ_3 do not depend on E_1. We have[7]

$$(8)\quad \begin{cases} \phi_1 = \sum_{\vec{g}} \dfrac{\phi(g^2)}{Q_z^2}\,; \qquad \phi_2 = 12 \sum_{\vec{g}} \phi(g^2)\,\Lambda(\theta,\alpha)\,\Gamma^2(\psi) \\ \phi_3 = \sum_{\vec{g}} \phi(g^2)\left\{ \dfrac{-\cos 2\psi}{Q_z^2} + 4D\,\Lambda(\theta,\alpha)\,\Gamma^2(\psi)\cos 2\psi + 2Q_z\,\Lambda(\theta,\alpha)\,\Delta(\psi)\sin 2\psi \right\}, \end{cases}$$

where

$$(9)\quad \begin{cases} \phi(g^2) = \dfrac{\left|F(l_1 l_2 l_3)\right|^2}{\pi^2 V n} \\ F(l_1,l_2,l_3) = \sum_{1}^{n}{}_j \dfrac{\left[Z_j - f_j(g^2)\right]}{g} \exp\left(-\frac{1}{2}A_j g^2\right) \exp\left[2\pi i(l_1 u_{1j} + l_2 u_{2j} + l_3 u_{3j})\right] \\ Q_z = q_z E_1 = \theta(g_2 \cos\alpha + g_3 \operatorname{sen}\alpha)\,; \qquad \Lambda(\theta,\alpha) = \dfrac{Q_z - D}{Q_z^4 g^2} \\ \Gamma(\psi) = q_\perp \cos\gamma = -g_2 \cos(\psi - \beta) + g_3 \sin(\psi - \beta) \\ \Delta(\psi) = (g_2^2 - g_3^2)\sin(2\psi - 2\beta) + 2 g_2 g_3 \cos(2\psi - 2\beta)\,; \end{cases}$$

$\cos 2\psi$ is given by eq. (5). The summation in the ϕ_i must be performed only for those reciprocal lattice points which lies on the coherence parabolo<u>id</u>; i.e. for the values of g_2, g_3 such that

$$(10)\qquad Q_z = D(1+U^2) - 2DU\Gamma(\psi) + \frac{g_2^2 + g_3^2}{2(1-x)}\,.$$

The set of permitted values of $\vec{g}$, as well as the functions ϕ_i depend thus on U and ψ.

The meaning of the symbols which were not defined is as follows. V is the volume of the basis lattice cell, which contains n atoms of atomic numbers Z_j at positions u_{1j}, u_{2j}, u_{3j} $(j = 1 \ldots n)$ (expressed as fractions of the sides a_1, a_2, a_3 of the cell). The triple of integers l_1, l_2, l_3 individuate a reciprocal lattice vector $\vec{g}$, whose components along $\vec{b}_1$, $\vec{b}_2$, $\vec{b}_3$ are $g_1 = 0$, g_2, g_3. $f_j(g^2)$ is the atomic scattering factor of the j^{th} atom in the unit cell. It has been pointed out[8] the necessity of using an efficient model for its computation. Extensive data of Hartree-Fock-Slater--Dirac calculations exist for free atoms in the form

$$(11)\qquad f(q^2) = \sum_{1}^{4}{}_i \alpha_i \exp(-\beta_i q^2) + c\,,$$

the coefficients α_i, β_i and c being widely tabulated[9]. For atoms bound in a crystal corrections should eventually be necessary[10].

A_j is in close relationship with the Debye-Waller thermal factor of the j^{th} atom. It was evaluated by Uberall[5] and Schiff[11] for a monoatomic as well as primitive cubic crystal. No method of calculating A_j exists for more complex cases. However it is sufficient to assume that a mean value A is appropriate; in general thermal factor is treated as an empirical constant in X-ray crystallography; an extensive tabulation has been made[12].

For the close analogy with X-ray scattering, we will call $F(l_1, l_2, l_3)$ the "structure factor". The function $\phi(g^2)$ depends only on the intrinsic characteristics of the crystal.

Functions $D^2\phi_1$ $D^3\phi_2$, and $D^2\phi_3$ depend on the ratio θ/D, not on θ and D separately. The form which is given the ϕ_i is the most convenient for folding the electron angular distribution.

Now a few words about the incoherent part $d\sigma^{(c)}$ of the differential cross section. Uberall's formulation essentially holds[13]; the only improvement made was the introduction of the more accurate expression (11), which, however, is not so important for the incoherent as for the coherent part is.

By adopting approximate eq. (2), integrations of eqs. (6) over U and ψ are made independent. Thus analytical integration over ψ from 0 to 2π gives rise to the following functions, in place of the ϕ_i of eqs. (8):

$$(12)\qquad \begin{cases} \chi_1(x) = 2\pi \sum_{\vec{g}} \dfrac{\phi(g^2)}{Q_z^2} \quad ; \qquad \chi_2(x) = 12\pi \sum_{\vec{g}} \phi(g^2)\, \Lambda(\theta, \alpha)\, g^2 \\ \chi_3(x) = -2\pi \sum_{\vec{g}} \dfrac{\phi(g^2)}{Q_z^4} \cos 2\varphi \ . \end{cases}$$

By using the Dirac δ-function, integration over U from 0 to U_o is obtained by performing the summation in eqs. (12) over values of $\vec{g}$ for which

$$(13)\qquad D \leq \theta\,(g_2 \cos\alpha + g_3 \operatorname{sen}\alpha) \leq D(1 + U_o^2).$$

The physical situation correspond to a round collimator, having a half aperture $U_o \ll 1$, placed in the bremsstrahlung beam at the angle U = 0. Other collimation geometries are of coarse possible; for instance, a small collimator placed at U = 1 with a suitable ψ favours the linear polarization but reduces the number photons collected. We systematically adopt the former collimation geometry, as the polarization can be made very high anyway by suitably choosing $\vec{g}$[4]. In this case the linear polarization is

$$(14) \qquad P = \frac{d\sigma_{\perp}^{(i)} - d\sigma_{\parallel}^{(i)}}{d\sigma^{(i)} + d\sigma^{(c)}} \quad ,$$

as the difference of the incoherent cross sections is vanishing. In eqs.(14) the symbols refer to cross section integrated over angles.

By using eq. (1) instead of (2), the integrations of coherent cross sections over angles are no longer independent and should be performed numerically, while for incoherent cross section integration is still analytical.

A typical result is shown in fig. 1 by the dashed curves. One can see that the left edge of each "line" is not as sharp as the right edge is. This is exactly the contribution given by the extra terms of eq. (1). If eqs. (12), (13) were used, the left corner had to fall abruptly like the right one[2]. By placing $U_o = \infty$ in eq. (13), the dot-dash curves of fig. 1 are obtained.

Let us now introduce the effects of electron multiple scattering as well as of the natural divergence of the beam. In order to do this we fold eqs. (6), (7), (8) with the normalized angular distribution function

$$(15) \qquad \begin{cases} G(\omega) = \dfrac{1}{\pi \omega_M^2(T)} \left\{ -Ei\left(-\dfrac{\omega^2}{\omega_o^2 + \omega_M^2(T)}\right) + Ei\left(-\dfrac{\omega^2}{\omega_o^2 + \omega_M^2(t_o)}\right) \right\} \\ Ei(-v) = -\displaystyle\int_v^{\infty} \frac{e^{-x}}{x}\, dx \, , \end{cases}$$

where ω represents the angle, measured in units of $1/E_1$, between the actual electron momentum $\vec{p}_1$ and the momentum $\vec{p}_1^{\,x}$ of the electron flying along the axis of the beam cone; T is the thickness of the crystal, measured in gr/cm^2;

$$t_o = \frac{M}{390\, Z^{1/3}(Z+1)} \quad ,$$

where M is the atomic mass, and Z is the atomic number (we consider one kind of atoms only; generalization for more than one atomic species is obvious);

$$\omega_M^2(t) = 0.6744\, \frac{Z(Z+1)}{M}\, t \ln \left\{ 1.531 \times 10^4\, \frac{Z^{1/3}(Z+1)}{M}\, \sqrt{T\, t_o} \right\} ,$$

where ω_M is a characteristic angle obtained from Moliere's theory of multiple scattering[14]; finally ω_o is the root mean square deviation of the angular distribution (assumed to be gaussian) due to natural divergence of the electron beam only. The electron scattering in the crystal was supposed to be incoherent; furthermore several other approximation were made in derivation of eq. (15).

The final cross sections are obtained by introducing the new inde

pendent variables ω, χ, U^{*}, and ψ^{*} in eqs. (9), and by considering the proper differential element. For instance, the following substitutions are performed

$$Q_z = \theta (g_2 \cos\alpha + g_3 \operatorname{sen}\alpha) - \omega\left[g_2 \cos(\beta - \chi) + g_3 \sin(\beta - \chi)\right]$$

$$U^2 = U^{*2} + \omega^2 - 2 U^{*} \omega \cos(\chi - \psi^{*}) \quad ; \tag{16}$$

here χ is the angle of planes $(\vec{p}_1^{\,*}, \vec{p}_1)$ and $(\vec{p}_1^{\,*}, \vec{\varepsilon})$; U^{*} and ψ^{*} mean U and ψ referred to $\vec{p}_1^{\,*}$. The final results are obtained by performing a triple numerical integration over ω, χ, and ψ^{*}, and by summing over those values of $\vec{g}$ for which U^{*}, as obtained from eqs. (10) and (16), is less than U_o (in this situation the emitted photon is collected from the collimator). A similar folding is also made for the incoherent cross section. The contribution of inelastic processes in which the atom is excited (bremsstrahlung due to atomic electrons) is of coarse incoherent. This is taken into account in an approximate way by adding the contribution of $1/Z$ times the incoherent cross section for the correspondent elastic process.

As far as the choice of the crystal is concerned, we sought among all crystals of the elements what is the one which gives the largest value of $\phi(g^2)/Z^2$ (see eq. (9)). The answer is that the best one is diamond; next comes beryllium, for which the maximum is only 5% smaller. On the contrary, the incoherent part $Z^{-2}\, d\sigma^{(c)}/dx$ is about 15% higher than for diamond is. This unfavours the ratio line height to background a bit. This ratio very unilikely is higher for crystals of compounds than for diamond and beryllium is.

The numerical result we present here are for a single crystal, of beryllium, which, apart from defects, is perhaps more easily obtained in form on thin plates than diamond is.

As regards the choice of the orientation, two alternatives are possible according to whether high line to background ratio or high polarization is required. The first one is obtained when the pancake intersects the plane $g_1 = 0$ along a high density reciprocal lattice row. The second alternative is obtained when the intersection contains a single reciprocal lattice point[4]. The latter has the advantage that the angle θ/E_1 can be chosen as large as 50 - 100 mrad; if a mosaic spread of some mrad exists for the axes of the crystal, its smearing out effect on the spectral lines is not so drastic as for small θ/E_1 is. For this reason we present results for the second alternative.

Beryllium crystal has a thermal factor A = 412 at room temperature[12], and a hexagonal close-packed structure. The basis cell has sides $a_1 = a_2 = 94.02$, at 120^{o} to each other and $a_3 = 147.44$, normal to both

a_1 and a_2. A fourth redundant axis $-(\vec{a}_1 + \vec{a}_2)$ is frequently used to display the hexagonal symmetry. The basis cell contains two atoms at positions 000 and 2/3 1/3 1/2. If we assume our coodinate system coincident with three suitable zone axes, namely $\vec{b}_1 \equiv [1\bar{2}10]$, $\vec{b}_2 \equiv [10\bar{1}0]$, $\vec{b}_3 \equiv [0001]$, the reciprocal lattice point 002, for which $\phi(g^2)$ is a maximum, may be the unique point contained within the pancake. This is accomplished for instance by taking $\alpha = 1.5^o$, $\theta = 602$, and $U_o = 0.4$, in such a way that the leading line of fig. 1 (dashed curve) has the upper edge at $x = 0.3$and a full width given by eq. (4). Minor "lines" of fig. 1 are due to reciprocal lattice points 004 and 006.

Specifically, fig. 1 was obtained for $mc^2 E_1 = 6$ GeV ($\theta/E_1 = 51.3$ mrad). The figure show both bremsstrahlung intensity $x\,(d\sigma/dx)/(Z^2 \sigma_o N)$ and linear polarization given by eq. (14) for $\beta = \alpha$, as a function of x up to the value $x = 0.6$. Both the dashed and the dot-dash curves are for no multiple scattering and no electron beam divergence, the former being obtained for $U_o = 0.4$, the latter for $U_o = \infty$ (no collimation). Incoherent background for the former case is $\sim 2\%$ of the line height, while polarization is 91%. By decreasing E_1 as well as by maintaining U_o constant, both incoherent background and line width remain unchanged, while the height of the coherent line is proportionally decreased. For small E_1, α should be increased to make θ/E_1 sufficiently small for our approximation to hold.

Continuous curve of fig. 1 shows the averaging effect of multiple scattering. We assumed beryllium crystal thickness $T = 9.25 \times 10^{-3}$ gr/cm^2 ($\omega_M(T) = 0.24$) and no electron beam divergence ($\omega_o = 0$). Polarization is not evaluated yet, only to save computer time. By extrapolation the maximum value of P is argued to be $\simeq 80\%$. In fig. 1 the full width at half maximum is indicated as Δx. It is the same as for the dashed curve is, but the energy distribution is of coarse more unfavourable and the maximum decreased.

In order to see whether such a beam may be used or not, the number of photons per MeV emitted by each electron is represented as a function of x in fig. 2. The continuous curve is computed in the previous conditions, while the dashed curve represents the opposite case in which angular divergence prevails on multiple scattering. We assumed $\omega_o = 0.5$, other conditions being unchanged. We have $\sqrt{\omega_o^2 + \omega_M^2(T)} = 0.56$ (see eq. (15)). Thus $\Delta x/x = 25\%$; the maximum is reduced by a factor 2.5.

We could have chosen a smaller U_o in order to increase the monochromaticity. By looking at fig. 2 we argue that this goal is made possible when the other conditions are the same as for the continuous curve are, while it is impossible for the dashed curve. Investigation of more specific cases as well as exact evaluation of polarization will be postponed to another occasion.

We conclude by saying that the typical number of 2×10^{-7} photons/ /MeV/electron of fig. 2 is largely sufficient for bubble chamber experiments,

if a beam intensity of, say, 10^{12} electron/second is available. (With this intensity, heating of the crystal by ionization loss is not a serious problem). The noticeable reduction of the soft component of the spectrum with respect to a conventional bremsstrahlung beam as well as the high value of the polarization can be conveniently used; but we cannot hope to obtain an effective monochromaticity of a few percent with this method, when a high photon beam intensity is required.

REFERENCES. -

(1) - G. Barbiellini, G. Bologna, G. Diambrini and G.P. Murtas, Phys. Rev. Letters 8, 454 (1962).
(2) - R. F. Mozley and J. De Wire, Nuovo Cimento, 27, 1281 (1963).
(3) - H. Überall, Zeits. f. Naturforschung, 17, 332 (1962).
(4) - G. Bologna, G. Lutz, H. D. Schulz, U. Timm and W. Zimmermann, Nuovo Cimento 42, 844 (1966).
(5) - H. Überall, Phys. Rev. 103, 1055 (1956).
(6) - M. May, Phys. Rev. 84, 265 (1951).
(7) - The first of eqs. (6), (7) and the first and second of eqs. (8) were obtained indipendently for the particular case $\alpha = \beta = 0$, $n = 1$ also by G. Barbiellini (private communication).
(8) - G. Bologna, G. Lutz, H. D. Schulz, U. Timm, and W. Zimmermann, V. Int. Conf. on high energy accelerators, Frascati, September 1965, Proceedings, p. 567.
(9) - D. T. Cromer, and J. T. Waber, Acta Cryst. 18, 104 (1965).
(10) - S. Gottlicher, and E. Wolfel, Zeits. f. Elettrochemie 63, 891 (1959).
(11) - L. I. Schiff, Phys. Rev. 117, 1394 (1960).
(12) - International tables for X-ray crystallography, Vol. III, sec. 3.3.5.1 (The Kynoch press, Birmingham, (1962)).
(13) - H. Überall, Phys. Rev. 107, 223 (1957).
(14) - W. T. Scott, Rev. Mod. Phys. 35, 231 (1963).